Sci. J. Fac. Sci. Minufiya Univ., Vol. XIV, 2000, 233-257

Structural Interpretation of the Airborne Magnetic Survey Data of Kharga-Dakhla Oases Area, Southern Western Desert, Egypt

BY

Abulhoda M. El-Sirafe*, Mahmoud M. El-Gamili, Moataz E. El-Manawy* and Mohamed A. El-Meliegy***

*Exploration Division, Nuclear Materials Authority, P. O. Box 530 El-Maadi, Cairo, Egypt

** Geology Department, Faculty of Science, El-Mansoura University, El-Mansoura, Egypt

ABSTRACT

The main aspects of the present study is to delineate the major tectonic features through analysis and interpretation of the potential anomalies in the studied area, also the basement configuration as delineated by qualitative and quantitative interpretation will be considered to throw more light on the subsurface geological picture and its structural framework.

In order to achieve the goal of the present work, the following steps were carried out : Reduction of aeromagnetic data to the north magnetic pole, trend analyses were carried out for the geophysical maps and surface lineaments in order to define the major surface and subsurface tectonic trends that affected the investigated area. Isolation of magnetic anomalies was carried out in order to identify residual local structures from those of regional nature. Depth computations for causative masses were carried out for the major magnetic anomalies in order to delineate adequately the structural relief of the magnetic basement surface and the structural deformations of the overlying sedimentary section and modeling of the possible causative geologic setting along some of the magnetic anomaly profiles.

The integrated information obtained from the different qualitative and quantitative interpretation techniques applied to magnetic data with all available geologic information were used to portray the basement configuration, to show the regional structural framework of the basement complex that have its influence on the overlying sedimentary section.

The major tectonic features on Kharga-Dakhla Oases area were delineated along three N-S magnetic modeled profiles beside magnetic depth estimations for the anomaly sources along 28 selected magnetic anomaly profiles using nine various techniques.

The basement shape map of the studied area shows five major tectonic provinces. These are the Great Dakhla Basin, East Kharga Basin, Abu Tartur Sub Basin, El-Kharga Uplift and Mid Basin Ridges. These structures seem to have a regional northerly dip. The study area shows also several NW- trending structures, which were modeled across three magnetic modeled profiles.

It was evident from the 2-D magnetic modeling that the modeled basement rocks show a wide range of magnetic susceptibility ranges between (1000-5800) x 10^{-6} c. g. s. units which reflect the great lateral variation in the petrographic composition of the crystalline basement rocks in the studied area.

INTRODUCTION

Location and Topography :

The area under investigation is located in the southern part of the Western Desert of Egypt (Fig. 1). This area, mainly includes the Kharga and Dakhla Oases, covers a total surface area of 55000 km^2. Geomorphologically, the area of study, as a part of the Western Desert of Egypt, may be considered as a part of the limestone Plateau which has been characterized throughout its recent history by arid climatic conditions.

Aim and Scope of Study :

The main aspects of the present geophysical study include the analysis and interpretation of the potential anomalies in the area under study to delineate the major and minor geophysical trends and their relation to the structural elements in the area. Also, the basement configuration as delineated by qualitative and quantitative interpretation will be considered to throw more light on the subsurface geological picture and its structural framework.

Different surface and subsurface geologic information were used to guide the interpretation of the geophysical data. The surface information were deduced from the geologic map of Egypt published by the Geological Survey of Egypt, 1981 (Fig. 5) and the map of the surface structural lineaments of the study area (Fig. 3) interpreted from LANDSAT-1 Satellite Images (El-Shazly et al., 1976). However, the subsurface information were collected from the available borehole data and previous publications, as the results of Zagorac et al. (1961).

In order to achieve the goal of the present work, the following steps were carried out :

1. Reduction of aeromagnetic data to the north magnetic pole.

2. Trend analyses were carried out for the geophysical maps and surface lineaments in order to define the major surface and subsurface tectonic trends that affected the investigated area.
3. Isolation of magnetic anomalies was carried out in order to identify the residual local structures from those of regional nature.
4. Depth computations for causative masses were carried out for the major magnetic anomalies in order to delineate adequately the structural relief of the magnetic basement surface and the structural deformations of the overlying sedimentary section.
5. Modeling of the possible causative geologic setting along some of the magnetic anomaly profiles.

The integrated information obtained from the various qualitative and quantitative interpretation techniques applied to magnetic data with all available geologic information were used to portray the basement configuration, to show the regional structural framework of the basement complex that have its influence on the overlying sedimentary section.

Airborne Magnetic Survey :

The total intensity aeromagnetic map of the study area (Fig. 6) was prepared by the Continental Sahara Company (CONCO), during November, 1976 to February, 1977. Compilation of the data was carried out by the Compagnie General de Geophysique. This magnetic survey has been flown along a system of N-S oriented flight traverses at spacing 1.5 km. This direction of flight lines was made perpendicular to the predominant magnetic trends in the area revealed from the previous regional surveys. The survey was conducted at a barometric altitude with a sensitivity 0.1 Nano Tesla (nT) of about 4500 ft using a proton precession magnetometer. Magnetic measurements were collected at a one second sampling interval. A doppler navigation system was used during the survey.

GENERAL GEOLOGICAL AND STRUCTURAL SETTING

I. GENERAL GEOLOGY

The Kharga-Dakhla Oases area is mainly covered by sedimentary rocks ranging in age from Jurassic to Quaternary. This sedimentary cover is locally interrupted by small scattered outcrops of Precambrian basement rocks mainly represented by granites and associated basic rocks in the vicinity of Abu Bayan locality in the southern part of the investigated area (Fig. 5).

II. STRUCTURAL SETTING

The structural elements of the Kharga-Dakhla stretch are the result of typical stable shelf tectonics. Faults and, to a lesser extent, large gentle folds are reflected on the surface and these indicate differential block movements in the basement. Most probably, the type and intensity of the resulting tectonics and deformations in the overlying strata are governed by the thickness and lithology of the rocks which differently constitute the sedimentary cover and particularly in its southern parts. Faults are the dominant tectonic feature and are of greater density and persistence. The southern part of the Kharga Oasis is the only sector in the Kharga-Dakhla stretch where outcrops of crystalline basement are found with a thin sedimentary cover and where the uparching of the basement rocks is pronounced. On the other hand, other areas to the west and northwest, including the Abu Tartour and Dakhla areas, the role of broad warpings and undulations is more prominent (Said, 1990).

FILTERING OF AEROMAGNETIC DATA

The total intensity aeromagnetic map of the investigated area was digitized on a north-south oriented square grid 2.5 X 2.5 km. The digitized magnetic data were fed into Microvax-II Computer System, where filtering operations including the reduction to the north magnetic pole, isolation of regional and residual anomalies using the band pass filter and the upward continuation techniques have been applied to the gridded aeromagnetic data using the available filtering software package of the Geophysical and Geological Mapping Center (G.G.M.C.) of the Nuclear Materials Authority (N. M. A.).

I. REDUCTION TO MAGNETIC POLE :

Magnetic interpretation is complicated by the fact that, magnetic anomalies associated with the different geologic bodies change their shape as the inclination of the earth's magnetic field changes. Because of this inclination variation, most magnetic anomalies show both a positive and a negative response. Reduction to pole filtering elimenates these inclination variation effects.

In the present study the reduction to pole filtering was applied in the frequency domain using Program of Fast Fourier Transformation of GEOSOFT Backage. The only input data required by program (R.T.P.) are the grid logical file parameters, declination, inclination and angle from true north and smoothed magnetic field data grid. Output is the reduced to pole magnetic field data grid, finally displayed on the reduced to pole magnetic map (Fig. 7).

II. ISOLATION OF MAGNETIC ANOMALIES :

A major step in the analysis of magnetic data is the process of isolating the observed anomaly pattern into a regional and residual components. This provides

the interpreter with valuable informations that helps in the delineation of the subsurface geological and structural setting in an area. The definition of "regional-residual" is purely subjective and arbitrary. It is best illustrated in a quatation from Nettleton (1976) : "the regional is what you take out in order to make what is left like the structure".

Construction of residual maps is one of the best known ways of interpreting magnetic data quantitatively. The isolation procedures are designed to separate broad regional variations from sharper local anomalies. In effect, the map is split into two parts : the regional and the residual maps. The residual focuses attention into weaker features which are obscured by strong regional effects in the original map.

In the present work, isolation of magnetic field anomalies was carried out using the band pass filter. Application of this filtering process was based mainly on the data obtained from the spectral analysis of the aeromagnetic data.

A. Spectral Analysis of Aeromagnetic Data :

Transformation of the magnetic data from the space domain to the frequency domain was done by applying the Fast Fourier Transformation (F F T) to the gridded magnetic data. We use the power spectrum of the magnetic signal to estimate the frequency content of the data. This permits us to filter out specific portions of the input signal (Fig. 4).

Depth computations performed on the computed radial power spectrum of the total aeromagnetic data of the area under investigation (Fig. 4) has revealed that, the magnetic signal originates from two average depth levels of 4.2 km and 2.5 km. The first depth level represents the average depth of the low frequency (long wavelength) magnetic anomalies which reflect the deep-seated (regional) geologic structures in the area. Meanwhile, the second depth level represents the average depth of the high frequency (short wavelength) magnetic anomalies which consequently reflects the shallower (local) geological structures in the area.

B. Application of the Band Pass Filter :

Isolation of the regional and residual magnetic anomalies in the studied area was carried out using the band pass filter technique. The band pass filter is comprised of a low pass filter and a high pass filter. To accomplish this type of filtering, operate in the same frequency domain grid twice, first using a high pass filter with one frequency cutoff, then using a low pass filter with another frequency cutoff, usually higher than the first. Regarding the present study the regional (deep-seated) magnetic anomalies have been isolated by applying the band pass filter to the gridded aeromagnetic data using 0.0 cycles / 500 m as a low cutoff frequency and 0.069 cycles/500 m as a high cutoff frequency. Where the residual (near-

surface) anomalies have been isolated using the band pass filter in the frequency range from 0.069 cycles / 500 m to 0.195 cycles / 500 m. Application of this type of filters has resulted in the construction of the regional and residual magnetic anomaly maps (Figures 8 and 9) respectively.

Application of Second Vertical Derivative :

So far we have demonstrated the principal methods of visualization of digital data as maps. We think that one of the great advantages of working with equally spaced data points (or profile data interpolated to an equal spacing) was the ability to apply digital filters and so affect various types of digital data processing. As with profile data, gridded data may also be processed by convolution with space-domain filters. In the case of gridded data, the filter operators themselves must also be two-dimensional arrays of values which are scanned along every row of data and, while centered over each data point in turn, a calculation is performed in which all the data points covered by the operator are involved and a new value is written to the corresponding position of the output grid.

For some applications, the second vertical derivative has the advantage of being non-directional. If we use the Laplacian potential field property that the sum of the second derivatives in the three orthogonal directions equals zero, then the sum of the estimates of the north-south and east-west second horizontal derivatives will equal (-1) (the second vertical derivative). Fig. (10) shows the regional magnetic-component filtered second vertical derivative map of the studied area.

METHODS OF DATA INTERPRETATION

I. ANALYSIS OF FREQUENCY DISTRIBUTION :

The trend analysis techniques were performed for the magnetic lineations traced from the various filtered anomaly maps (Figs. 11 and 12) as well as photolineations interpreted from LANDSAT-1 Satellite Images by El-Shazly et al., 1975 (Fig. 13). The main purpose of this investigation is to define the prevailing tectonic trends affecting the study area as reflected on the various geophysical and photolineations maps and to check the relation which might exist among the deep-seated (regional), the near-surface (residual) and the surface (photolineations) tectonic trends.

A. Surface Lineation Trend Patterns :

Statistical trend analysis of the photolineations interpreted from the LANDSAT-1 Satellite Images of the study area by El-Shazly et al., 1975 (Fig. 3), showed that the area under investigation has been affected by three fracturing trends namely : the NNE, E-W and WNW trends. These fracturing trends are shown up on the surface lineation rose diagram (Fig. 13) as three peaks centered at

N 10° E (NNE), N 85° E (E-W) and N60°W arranged in a decreasing order of magnitude. However the NNE trend has a distinct higher statistical significance if compared with other minor trends (Meshref, 1982). Surface E-W fracturing trend is interpreted to be genetically contributed to the rejuvenation of older tectonic movement along deep seated Precambrian E-W tectonic trend, since this trend was a remarkable good development on the regional and residual magnetic trends frequency plots (Figs. 11 and 12). On the other hand, the WNW trend is interpreted to be due to the shear couple force affected the Red Sea region (Meshref and El-Sheikh, 1973).

B. Regional Magnetic Trend Patterns :

Statistical analysis of trends of regional magnetic anomalies and gradients revealed that the area under investigation seems to be highly affected by four significant tectonic trends of regional nature. These trends most probably complicated the deeply buried, Precambrian crystalline basement rocks as well as the overlying early Paleozoic rocks. These tectonic trends are shown up on the regional magnetic lineaments rose diagram (Fig. 11) as four well-developed peaks that trend N45°E (NE), N05°E (N-S), N65°E (ENE) and N85°E (E-W) arranged in a decreasing order of magnitude. However the NE trend shows a distinct higher statistical significance if compared with the other three trends. These magnetically interpreted tectonic trends are believed to be associated with the older and most prevailing subsurface tectonic structures in the studied area.

The E-W trend is considered by El-Shazly (1966) as the oldest tectonic trend affecting the Egyptian basement rocks where it started by the Late Geosynclinal Stage during the Precambrian Orogeny.

The regional magnetic map (Fig. 8) shows separate individual anomalies of WNW trend within the anomalous ENE zones. This may suggest an older age for the Causative source for the WNW anomalies that seem to be truncated by younger ENE (Syrian Arc) trending anomalies.

C. Residual Magnetic Trend Patterns :

The comparative inspection of the residual and regional magnetic trend patterns revealed that, the residual (local) magnetic trends seem to be governed to a large extent by the deep regional magnetic trends. This interpretation may be confirmed by the fact that both the N-S and E-W regional magnetic trends are well expressed on the rose diagram (Fig. 12) which shows the frequency distribution of the residual magnetic trends as two well-developed major peaks that trend N 05° W and N 85° E respectively. Meanwhile it was noticed that both the NE and ENE tectonic trends show up as a minor peaks on the rose diagram of the residual magnetic trends.

The two-dimensional autocorrelogram of the residual magnetic-component map (Fig. 9) shows a distinctly elongate feature of contours in almost east-west direction, characterizing the principal direction trend. Less striking than the principal trend but of comparable importance are the well-developed regions of low values located to the northeast and southwest. If lines are drawn through similar features on the plot, two groups of intersecting trends (N-S and NE) are found. (Fig. 12) shows the trend directions determined from the autocorrelogram (Fig. 9). The dominant (principal) direction is indicated by heavier lines (denoted P) while the secondary trends which are interest at approximately 45° are indicated by a dashed lines (denoted S1 and S2). It is believed that the major axis of the stress ellipsoid responsible for the creation of the interpreted tectonic trends is perpendicular to the principal trend marked P.

II. DEPTH COMPUTATION RESULTS :

The depth to the anomaly sources distributed in the mapped area were computed using several methods and techniques. The results of these computations for the chosen isolated clean anomalies are shown in Table (1). These results are reduced to the mean Sea level. The depths computed for the magnetic sources using the different methods, are averaged together with the corresponding depths computed by the spectral analysis technique.

The inspection of depth computation results (Table 1) shows a good coordination with the borehole data. This is clearly shown at the location of the boreholes B-14 and WSD (Fig. 15) which are crossed by the magnetic anomaly profiles 18 and 7-respectively. Also Mut-3 well was drilled in the vicinity of the magnetic modeled cross-section A- A' that gives a good agreement with the computation results.

Generally, depth computations for the area under study revealed that, the depth to the basement surface in the area of study ranges from 0.50 to 0.22 km. The average depth to the basement surface in El-Kharga Oasis is about 0.60 km. The average depth for the magnetic basement surface as delineated from the computation results in addition to the depths obtained from the drilled holes and the magnetic modeling technique are used to construct a magnetic basement tectonic map for the area of study (Fig. 15).

Also it is shown from depth computation results that there is a general dip of the basement surface towards the north and west directions where there is some granitic outcrops at G. Abu-Bayan El-Qebli and G. Abu-Bayan El-Bahari and continued west with a depth computation values 480 m below sea level at El-Kharga Uplift and +190 m above sea level (anomalies Nos. 18 and 7, Table 1). To the north the depth to the basement surface reached up to 2200m below sea

level at Abu-Tartur Basin and 1850 m at Dakhla Basin (anomalies Nos. 8 and 10, Table 1).

III. BASEMENT SHAPE MAP:

Results obtained from the qualitative and quantitative interpretation techniques applied to the aeromagnetic data of the studied area have been used in conjunction with all available surface as well as subsurface geological information to construct the tectonic map of the area (Fig. 14). This map illustrates the structural configuration of the buried magnetic basement rocks. Close inspection of this map illustrates the following major structural features : The Great Dakhla Basin, East Kharga Basin, El-Kharga Uplift, Oweinat Uplift and the Mid Basin Ridges.

A. The Great Dakhla Basin :

This structurally controlled sedimentary basin occupies the central part of the study area. It is a triangular-shaped with its top at the extreme southern border of the area. It is bounded from the west and southwest by the Oweinat Uplift and El-Kharga Uplift from the east. It seems that the Dakhla Basin extends to the northwest beyond the limits of the studied area. This is in agreement with Said (1990) who mentioned that "the depocenter of the Dakhla Basin fall under the Great Sand Sea and extends further to the northwest, beyond the limits of the studied area till the southern reaches of the Farafra Oasis". Magnetic depth estimates as well as quantitative two-dimensional magnetic sedimentary section within the outlined Dakhla Basin ranges from 1200 to 2200 m.

The deepest part of the basin was delineated around Gabal Abu-Tartur (Fig. 14) where the magnetic basement reaches its maximum depth (2200 m). This local depocenter has given the name Abu-Tartur Sub-Basin. This Sub-Basin occupies the northeastern portion of the Dakhla Basin and is bounded from the east by El-Kharga Uplift and from the northwest direction by one of the two elongated mid basin ridges I and II (Fig. 14) which cut across the major Dakhla Basin in almost E-W to NE direction. Regarding hydrocarbons exploration within the great Dakhla Basin, mid basin ridges I and II are recommended as a good exploration targets.

Said (1990) mentioned that the sedimentary cover in the Dakhla and Kharga areas represents the in fill of the Dakhla Basin from Late Triassic to Early Eocene. He also added that, Late Jurassic Sediments are the oldest recorded in the stretch, as revealed by surface investigations and the available subsurface drilling data.

B. East Kharga Basin :

The East Kharga Basin occupies the extreme eastern portion of the studied area (Fig. 14) bounded from the west by El-Kharga Uplift. It seems that this basin extends further to the east beyond the limits of the area under consideration. East

Kharga Basin is sometimes referred to in the literature as Assiut-Upper Nile Basin (Said, 1990). Said (ibd) reported that two sedimentary basins exist on the northward sloping Aquifer Craton. These are the Dakhla Basin on the west and Assiut-Upper Nile Basin on the east, with the Kharga Uplift in between.

Said (1990) mentioned that, to the east of El-Kharga Uplift, the present plateau area extending to the Nile Valley as occupied by a shallow depression (East Kharga Basin) characterized by relatively shallow marine sediments of Late Cretaceous to Early Eocene age and presumable by thin development of older Mesozoic strata.

C. El-Kharga Uplift :

El-Kharga High is featured at the eastern portion of the studied area (Fig. 14). It is a N-S striking high basement structure delimits the eastern rim of the whole Dakhla Basin and separates it from the adjacent East Kharga Basin (Assiut-Upper Nile Basin). Wells drilled over this structural uplift revealed that the depth to the Precambrian basement rocks oscillates between 400 and 700 meters. On the other hand, the modeled magnetic profile C-C′ (Fig. 18) demonstrates that the crystalline rocks forming this high basement structure posses a relatively high magnetic susceptibility (4500×10^{-6} c.g.s. unit) which may indicate that these relatively basic igneous rocks were introduced into the relatively acidic rocks (1000×10^{-6} c. g. s. unit) forming the surrounding basinal area. This basin is interrupted by a NE-trending high structures referred to in this study as the mid basin ridges I and II (Fig. 14).

Correlative inspection of the interpreted basement tectonic map of the area (Fig. 15) with both the geologic and topographic maps (Figs. 5 and 2) showed clearly that El-Kharga Depression can be regarded as representing the surface topographic expression of the buried El-Kharga Basement Uplift, where the tectonic and differential erosion factors played an important role in configurating this high basement structure.

D. Oweinat Uplift :

Oweinat Uplift occupies the southern western portion of the studied area (Fig. 14) and it seems that this high basement structure extends further to the south and west beyond the limits of the area. The Oweinat Uplift delineates the western rim of the Great Dakhla High to the east. Qualitative interpretation of the magnetic relief associated with this high structure indicated the presence of a number of low frequency high amplitude positive magnetic anomalies which may reflect intruded deep-seated igneous bodies (igneous plugs) of relatively high magnetic susceptibility.

IV. MODELED MAGNETIC PROFILES :

A. Magnetic Profile No. A-A' :

Results of the two-dimensional modeling of this magnetic profile are shown on Figure (16). The upper half of the figure shows the observed regional magnetic profile along profile A-A′ as traced from the filtered regional magnetic map (Fig. 8). The observed magnetic profile is shown as a solid line, while the computed magnetic effect due to the assumed basement configuration; is presented as a dashed line. The reason that modeling was carried across a longer profile than that traced from the regional magnetic map, is to get rid of the edge effect at both ends of the modeled profile. Along the X-axis of this profile location of the drilled well Mut-3 is projected.

The basement configuration along profile A-A′ "as shown on the lower half of the Figure No. 16" is composed of five geologic bodies represented by nine polygons. These bodies from north to south have the following susceptibilities 0.001, 0.0026, 0.001, 0.0015, 0.001, 0.0045, 0.001, 0.0012 and 0.001 c. g. s. units. Here follows is a comparison between the estimated basement depth as deduced from magnetic modeling and that obtained from drilling data at the location of the drilled well Mut-3 along profile A-A′ where depth from drilling equal > 1.050 km and the estimated basement depth from modeling equal 1.700 km. This contraversy may be attributed that the possibility that, the proposed magnetic basement surface is lower than the active basement surface reached in the drilled well. It is noticed that the magnetic susceptibility assumed to the basement blocks range from (1300-5000) x 10^{-6} c. g. s. units. Body of k2 with magnetic susceptibility 0.0026 c. g. s. units may be of leucite rocks or leucite-quartz-diorite, moreover bodies of (k3 and k5) with magnetic susceptibilities 0.0013 and 0.0015 c. g. s. units may be abyssal naphelites and eruptive naphelites or peridotite or andesites.

Body of k4 with magnetic susceptibility 0.0045 c.g.s. units may be considered as a basic intrusion within the basement may be of (pyroxenites). It must be taken in consideration that all these rocks intruded the main surface of the granitic basement of magnetic susceptibilities 0.001 c. g. s. units.

B. Magnetic Profile No. B-B' :

Cross-section No. B-B′ (Fig. 17) shows almost the same major basement blocks as in cross-section No. A-A′. The magnetic susceptibility values given for these basement blocks along this cross-section are not vary greatly from their corresponding values along cross-section A-A′. There are five geologic bodies represented by seven polygons. These bodies from north to south have the following susceptibilities 0.0010, 0.0015, 0.0010, 0.0050, 0.0010, 0.0013 and 0.0010 c.g.s. units (Fig. 17). Body of k2 of magnetic susceptibility 0.0050 c.g.s. units may be the same of body of k4 in cross-section A-A′ which may be of

pyroxenites too. Consequently, body of magnetic susceptibility k4 = 0.0013 just like body of magnetic susceptibility k5 = 0.0013 in profile A-A′ of eruptive naphelites, peridotites or andesites. Moreover, body of k3 = 0.0015 c. g. s. units in this profile may be the same body of k2 = 0.0026 c. g. s. units of leucite rocks or leucite-quartz-diorite. Body of k2 = 0.0050 c. g. s. units may be considered as a basic intrabasement intrusion deep rooted infinite monopole dyke where its amplitude up to 260 nT on the regional magnetic map (Fig. 8).

C. Interpreted Cross-Section No. C-C′ :

This profile shows almost the same behavior as in profiles Nos. A-A′ and B-B′. It is believed that this higher area along this profile C-C′ (Fig. 18) can be related to the shallower basement depth to the southern part near Baris. Meanwhile, the northern part of the higher area which accompanied by low magnetic anomalies are probably caused by the presence of low structural parts of the underlying basement. In the southern part there is two magnetic anomalies which are associated with two intrusions of magnetic susceptibilities (k3 = 0.0012 and k4 = 0.0012 c. g. s. units) and the body k3 is shallower in depth than k4 and both of them may be of andesite. On the other hand body of k2 with a magnetic susceptibility 0.0045 c. g. s. may be of pyroxenites.

As a result of quantitative magnetic modeling the following conclusions were obtained :

1. The major interpreted tectonic features in the studied area were delineated and confirmed along the three N-S modeled profiles A-A′, B-B′ and C-C′ (Fig. 15). There tectonic features are mainly represented by the Great Dakhla Basin, the East Kharga Basin (Assiut-Upper Nile Basin), El-Kharga high, Mid Dakhla Basin Ridges and Oweinat High. These structures seem to have a regional northerly dip.
2. It was evident that the modeled basement rocks show a wide range of magnetic susceptibility ranges between $(1000\text{-}2800)\times10^{-6}$ c.g.s. units which indicates a great lateral variation in the lithologic composition of the crystalline basement rocks across the studied area.
3. The high structures within the studied area are generally associated with basement blocks of higher magnetic susceptibility values as in the Northern Dakhla Basin, the Mid Basin Ridge and El-Kharga High where the susceptibility of the basement rocks forming these high structures ranges between $(1300\text{-}5800)\times10^{-6}$ c. g. s. This suggests that these structures may have related to intrusion of mantle type basic material intruded into the crystalline basement rocks. Meanwhile, the major basinal areas seem to be associated with a relatively acidic basement rocks.

4. Modeling of regional magnetic profiles shows only the regional tectonic framework, but in order to interpret adequately all the detailed structures within an area, the filtered residual magnetic anomalies should be considered as a prequisite for modeling the residual magnetic anomalies associated with local geologic structures.

SUMMARY AND CONCLUSIONS

Results obtained from the qualitative and quantitative interpretation techniques applied to the aeromagnetic data of the studied area have been used in conjunction with all available surface as well as subsurface geological information to construct the tectonic map of the area which illustrates the structural configuration of the buried magnetic basement rocks and illustrates the following major structural features : The Great Dakhla Basin, East Kharga Basin, El-Kharga Uplift, Oweinat Uplift and the Mid-Basin Ridges.

As a result of quantitative magnetic modeling the following conclusions were obtained :

1. The major interpreted tectonic features in the studied area were delineated and confirmed along the three N-S modeled profiles Nos. A-A′, B-B′ and C-C′ (Fig. 15). Three tectonic features are mainly represented by the Great Dakhla Sub-Basins, the Eocene Kharga Basin (Assiut-Upper Nile Basin), El-Kharga high, Mid Dakhla Basin Ridges and Oweinat High. These structures seem to have a regional northerly dip.

2. It was evident that the modeled basement rocks show a wide range of magnetic susceptibility ranges between (1000-2800) x 10^{-6} c. g. s. units which indicates a great lateral variation in the lithologic composition of the crystalline basement rocks across the studied area.

3. The high structures within the studied area are generally associated with basement blocks of higher magnetic susceptibility values as in the Northern Dakhla High, the Mid Basin Ridge and El-Kharga High where the susceptibility of the basement rocks forming these high structures ranges between (1300-5800) x 10^{-6} c.g.s. This suggests that these structures may have related due to intrusion of mantle type basic material into the crystalline basement rocks. Meanwhile, the major basinal areas seem to be associated with a relatively acidic basement rocks.

4. Modeling of regional magnetic profiles shows only the regional tectonic framework, but in order to interpret adequately all the detailed structures within an area, the filtered residual magnetic anomalies should be considered as a prequisite for modeling the residual magnetic anomalies associated with local geologic structures.

The major tectonic features on Kharga-Dakhla Oases area were delineated along three N-S magnetic modeled profiles beside magnetic depth estimations for the anomaly sources along 28 selected magnetic anomaly profiles using nine various techniques.

The basement shape map of the studied area shows five major tectonic provinces. These are the Great Dakhla Basin, East Kharga Basin, Abu-Tartur Sub Basin, El-Kharga Uplift and Mid Basin Ridges. These structures seem to have a regional northerly dip. The study area shows also several NW- trending structures, which were modeled across three magnetic modeled profiles.

It was evident from the 2-D magnetic modeling that the modeled basement rocks show a wide range of magnetic susceptibility ranges between (1000-5800) x 10^{-6} c. g. s. units which reflect the great lateral variation in the petrographic composition of the crystalline basement rocks in the studied area.

REFERRENCES

Continental Sahara Company (November, 1976) : Total Magnetic Intensity map.

El-Shazly, E. M. (1966) : Structural development of Egypt, U. A. R. ; Geological Society of Egypt, Program and Abstracts, pp. 31-38.

El-Shazly, E. M., El-Ghawaby, M. A. and Assaf, H. S. (1975) : Contribution to geology and structural analysis of the Central Eastern Desert of Egypt, Egypt. J. Geol.

El-Shazly, E. M., Abdel Hady, M. A., El-Kassas, I. A., Salman, A. B., El-Amin, H. and El-Shazly, M. M. (1976) : Geology of Kharga-Dakhla Oases area, Western Desert, Egypt from Landsat-1 Satellite Images, Remote Sensing Center, Cairo, Egypt.

Geological Survey of Egypt (1981) : Geological Map of Egypt, Scale 1: 2,000,000 published by the Geological Survey of Egypt.

Ghobrial, M. G. (1965) : The structural geology of the Kharga Oasis. Geological Survey and Mining Resources Department, Cairo, Egypt.

Meshref, W. M. (1982) : Regional structural setting of Northern Egypt. E. G. P. C. 6th Exploration Seminar, Cairo, Egypt.

Meshref, W. M. and El-Sheikh, M. A. (1973) : Magnetic tectonic trend analysis in Northern Egypt. V. 17, No. 2, pp. 179-184.

Nettleton, L. L. (1976) : Gravity and magnetic in oil prospecting. Mc Graw-Hill Book Co., New York.

Said, R. (1990) : The geology of Egypt. Balkema Publishers, Rotterdam, Netherlands, 734 p.

Zagorac, Z., Rimac, I., Febic, K. and Kovacevis, S. (1961) : Report on gravimetric and geologic surveys, Kharga and Dakhla Oases, 1960-1961. Report by (Geophizika) Zagreb, Yogoslavia, to Gen. Des. Develop. Org., Cairo, Egypt.

Table (1) : Results Obtained from the Application of Magnetic Depth Estimation Methods, Kharga-Dakhla Oases area, Southern Western Desert, Egypt

Profile No.	Straight Slope Method (1949)	Peter's Method (1949)	Piatinsky Method (1950)	Bean's Method (1966)	Durantny And Krs (1963)	Sokolov Method (1964)	Logacheav Method (1968)	Koulomzine et al. Method (1970)	Nakhla Method (1970)	Spectral Analysis Technique	Average Depth (km)	Depth Sea Level (m)
1	1.20	1.40	1.86	1.54	.....	2.13	2.25	....	....	....	1.920	420
2	1.50	1.56	2.20	1.76	.....	2.75	2.18	....	....	....	2.376	818
3	2.50	2.89	1.93	2.17	1.72	1.88	1.63	....	....	....	2.370	870
4	1.25	2.30	1.20	1.84	1.17	1.43	2.00	....	1.27	....	2.150	650
5	.2.25	2.80	2.30	2.08	1.22	2.12	1.88	2.49	1.48	....	2.200	700
6	2.20	4.80	3.00	3.06	.....	3.50	....	3.00	....	....	2.480	980
7	3.00	3.53	3.02	2.50	.....	2.60	....	....	2.85	2.40	2.700	1200
8	3.75	4.30	4.60	4.58	....	3.10	4.05	....	2.10	2.20	3.720	2220
9	2.30	2.30	.....	3.01	....	2.86	1.77	3.12	....	3.26	2.900	1500
10	3.25	3.10	3.42	3.51	....	3.30	3.55	3.40	3.26	....	3.355	1256
11	1.10	1.70	0.83	1.73	2.00	0.94	0.87	1.83	1.20	1.08	....	180
12	2.00	2.10	....	4.13	....	4.20	2.62	4.00	2.15	3.02	2.210	720
13	2.45	4.20	4.40	1.82	2.20	3.25	3.00	3.33	....	1.19	2.100	1200
14	3.25	4.50	3.38	3.15	4.00	2.12	1.00	5.40	5.40	2.45	2.870	1370
15	2.80	3060	1.01	2.35	3.50	1.65	2.12	5.30	2.70	1.00	2.800	1300
16	3.60	4.30	2.80	.....	2.10	3.20	2.17	4.40	....	1.40	2.950	1150
17	3.64	.....	0.35	.....	....	4.06	2.50	....	6.17	1.76	2.020	720
18	2.03	2.00	.....	2.18	2.13	2.25	1.50	2.16	1.57	2.10	1.987	487
19	2.50	4.50	4.10	2.20	....	3.40	2.00	1.80	....	1.78	2.050	550
20	3.25	2.60	2.10	1.50	2.18	1.00	2.00	3.08	....	2.46	2.310	010
21	2.37	2.00	1.90	1.90	2.02	2.06	2.03	2.60	....	4.20	2.200	700
22	1.50	1.70	0.93	1.06	1.06	1.06	1.25	2.20	1.08	2.20	1.310	100
23	3.30	3.20	2.00	2.33	1.33	2.40	1.87	....	1.73	1.90	1.750	250
24	3.70	4.10	2.28	2.61	....	3.60	....	4.40	2.25	1.83	2.000	830
25	3.25	3.60	3.00	.....	1.50	2.93	2.25	2.70	1.68	....	2.810	1310
26	4.70	5.00	5.00	....	2.10	4.25	4.10	....	....	....	.....	.....
27	2.50	3.70	2.00	1.90	1.91	2.12	3.10	.....	2.53	....	2.600	1100
28	3.30	3.20	1.80	2.20	0.30	2.25	2.50	3.60	....	....	2.800	1200

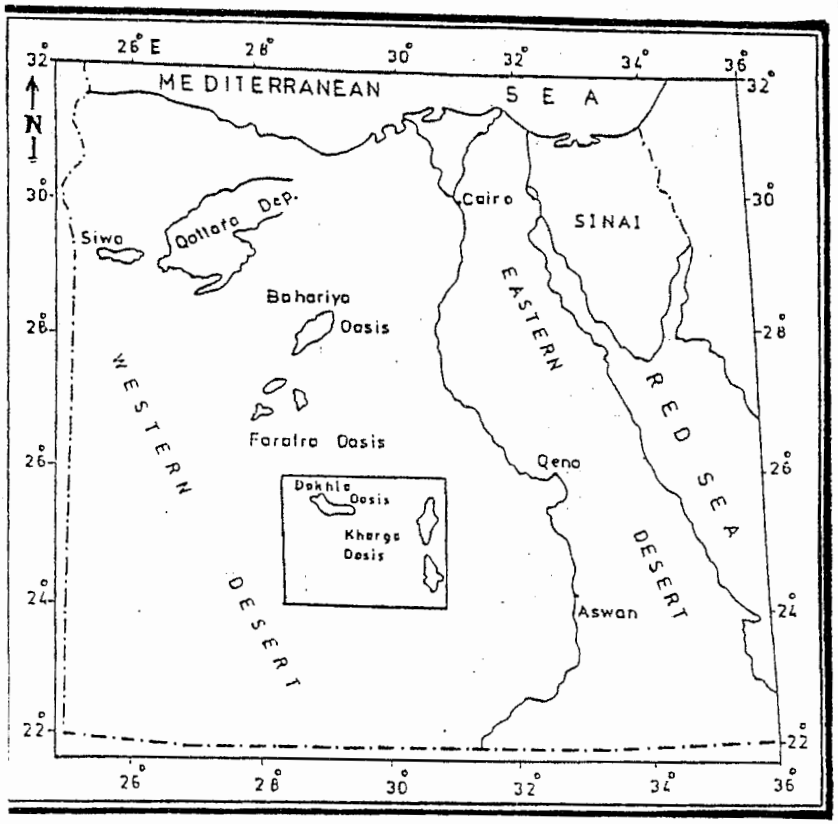

Fig. (1) : Location Map of Kharga-Dakhla Oases area, Southern Western Desert, Egypt

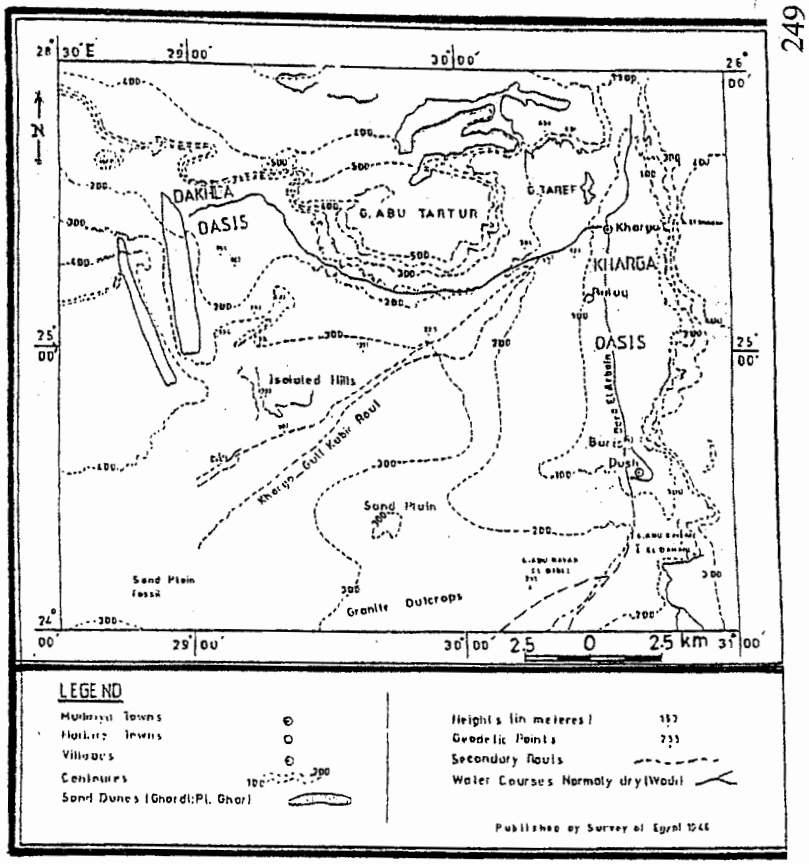

Fig. (2) : Map Showing the Main Topographic Features of Kharga-Dakhla Oases area, Southern Western Desert, Egypt

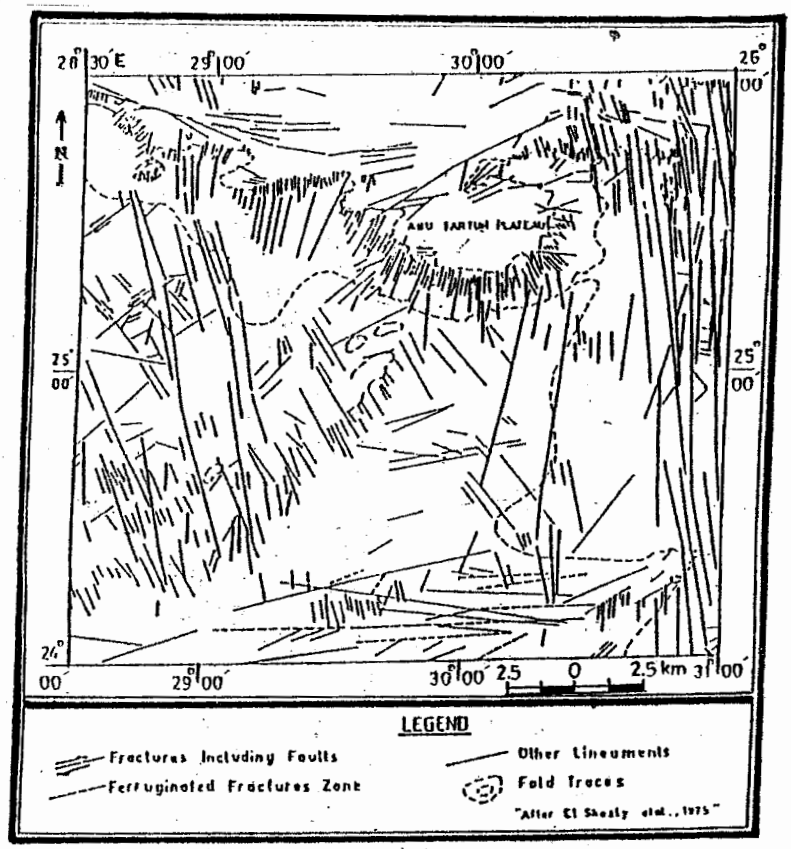

Fig. (3) : Structural Lineation Map of Kharga-Dakhla Oases area, Southern Western Desert, Egypt (Interpreinted from LANDSAT-1 Satellite Images)

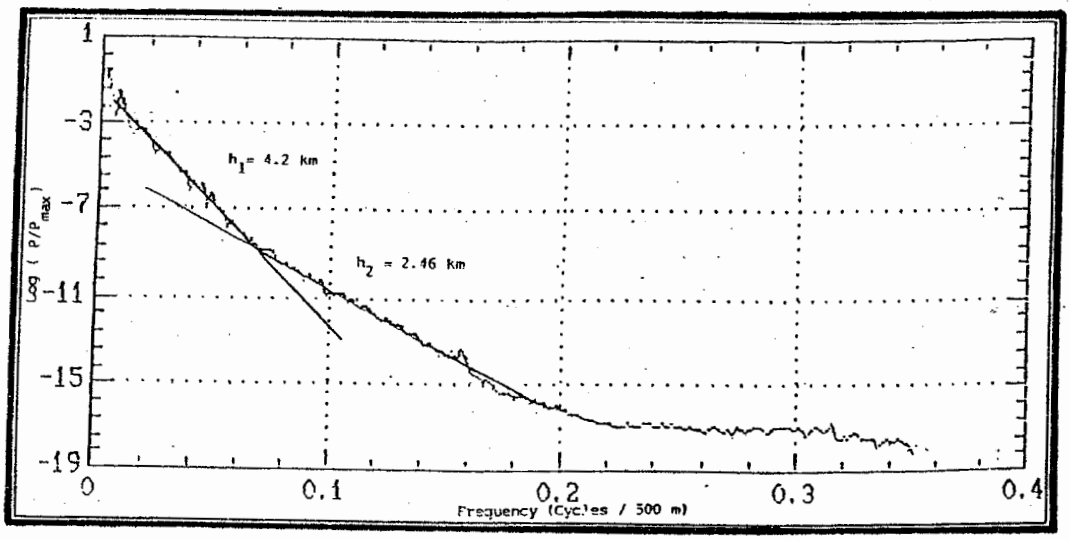

Fig. (4) : Computed Radial Power Spectrum of the Total Intensity Aeromagnetic Map, Kharga-Dakhla Oases area, Southern Western Desert, Egypt

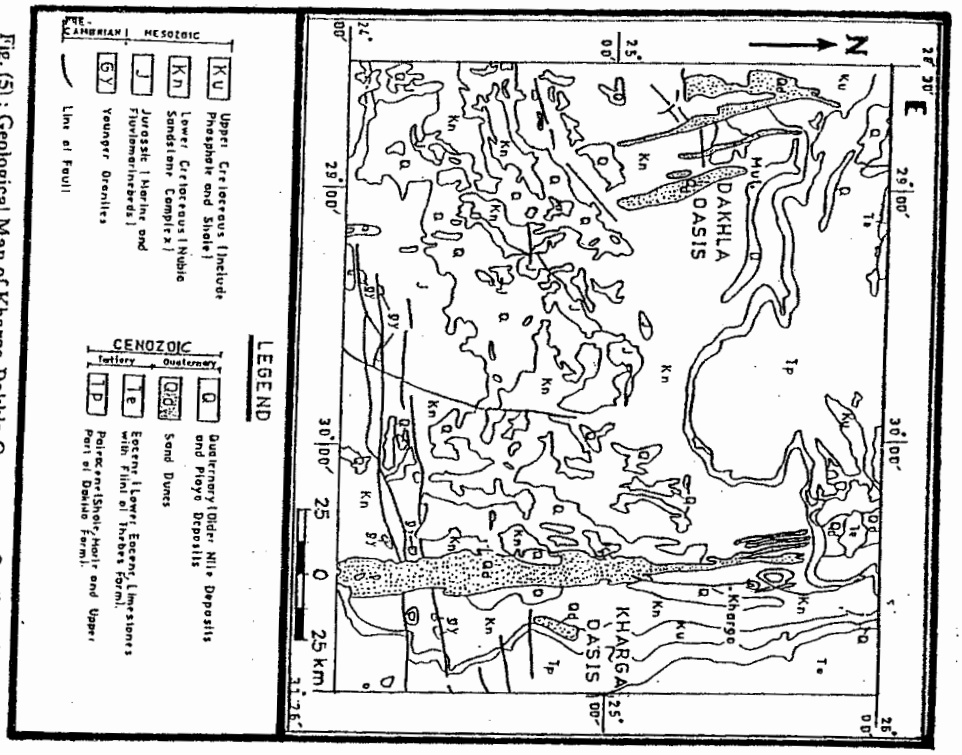

Fig. (5) : Geological Map of Kharga-Dakhla Oases area, Southern Western Desert, Egypt (after the Geological Survey of Egypt, 1981)

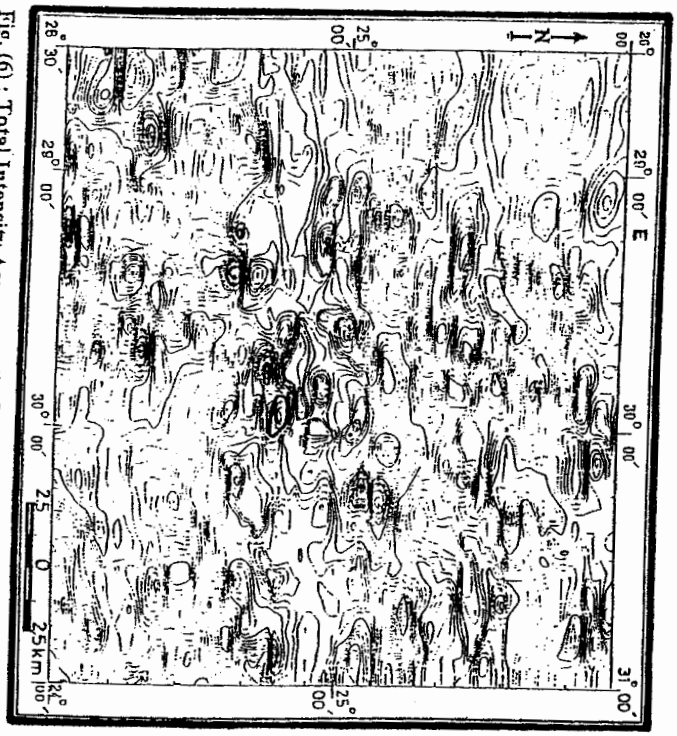

Fig. (6) : Total Intensity Aeromagnetic Contour Map of Kharga-Dakhla Oases area, Southern Western Desert, Egypt

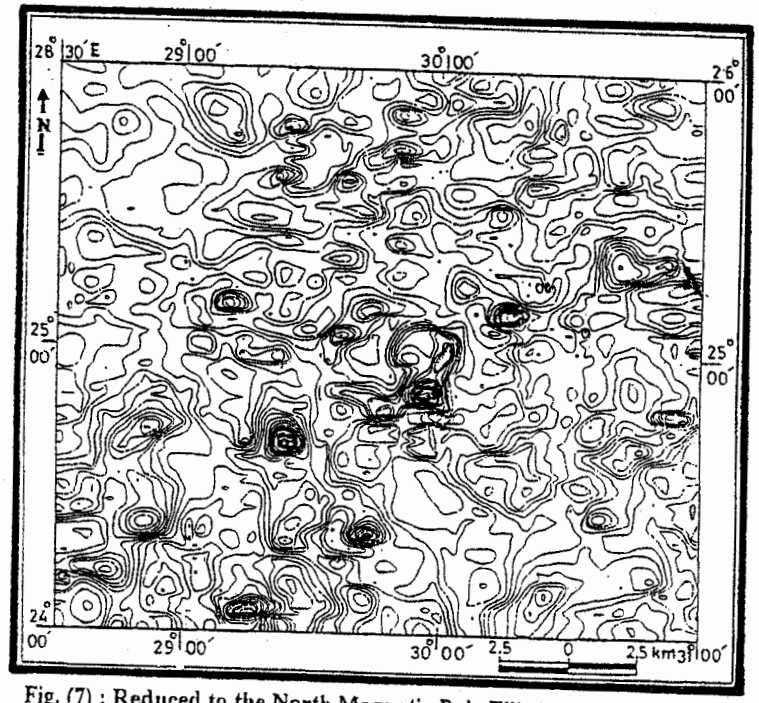

Fig. (7) : Reduced to the North Magnetic Pole Filled Colored Contour Map of Kharga-Dakhla Oases area, Southern Western Desert, Egypt

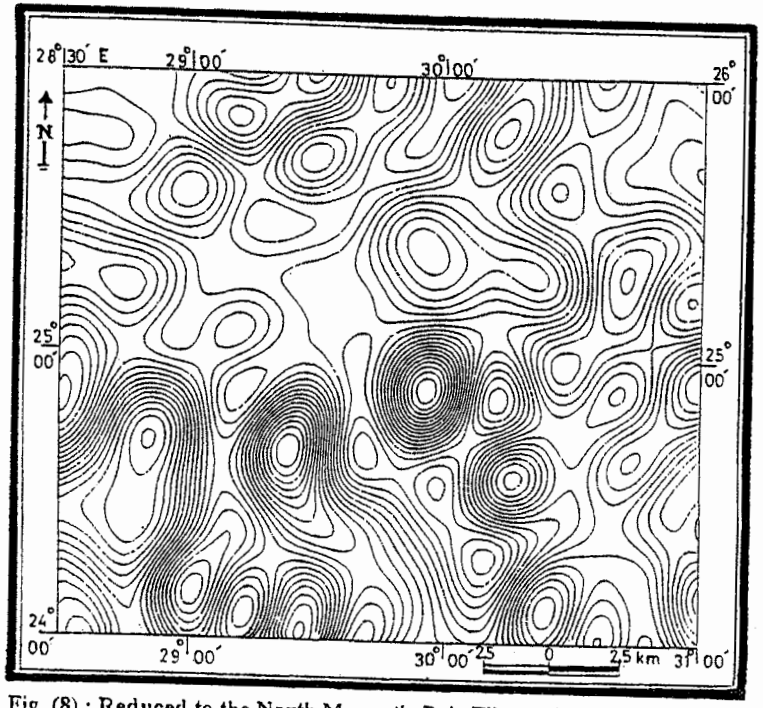

Fig. (8) : Reduced to the North Magnetic Pole Filtered Regional Magnetic Component Filled Colored Contour Map of Kharga-Dakhla Oases area, Southern Western Desert, Egypt

Low Cutoff Frequency = 0.000 Cycle / 500 m
High Cutoff Frequency = 0.069 Cycle / 500 m
Average Depth = 4.200 km

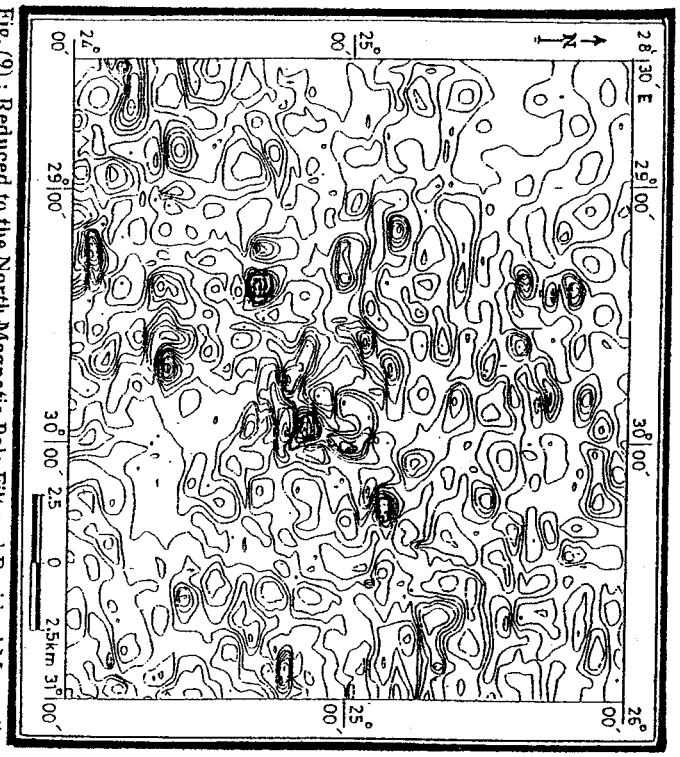

Fig. (9) : Reduced to the North Magnetic Pole Filtered Residual Magnetic Component Filled Colored Contour Map of Kharga-Dakhla Oases area, Southern Western Desert, Egypt

Low Cutoff Frequency = 0.069 Cycle / 500 m
High Cutoff Frequency = 0.195 Cycle / 500 m
Average Depth = 2.460 km

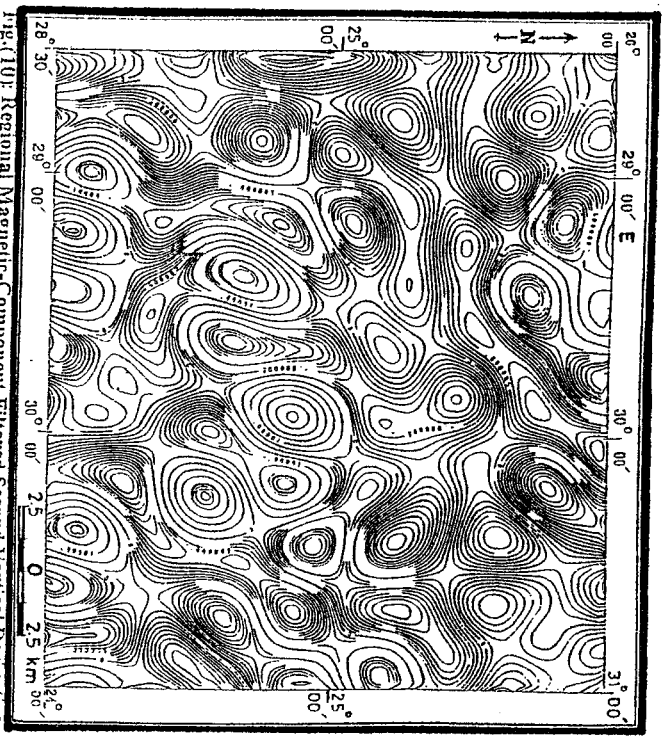

Fig. (10): Regional Magnetic-Component Filtered Second Vertical Derivative Filled Colored Contour Map of Kharga-Dakhla Oases area, Southern Western Desert, Egypt

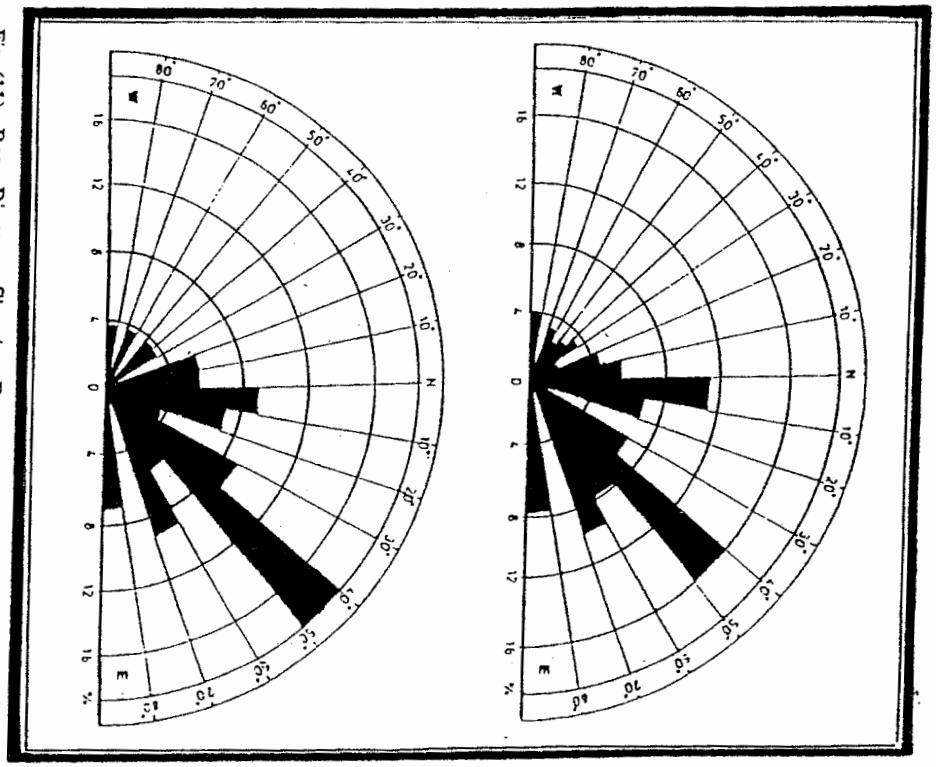

Fig. (11) : Rose Diagram Showing Frequency Distribution of Regional Magnetic Lineations in Kharga-Dakhla Oases area, Southern Western Desert, Egypt

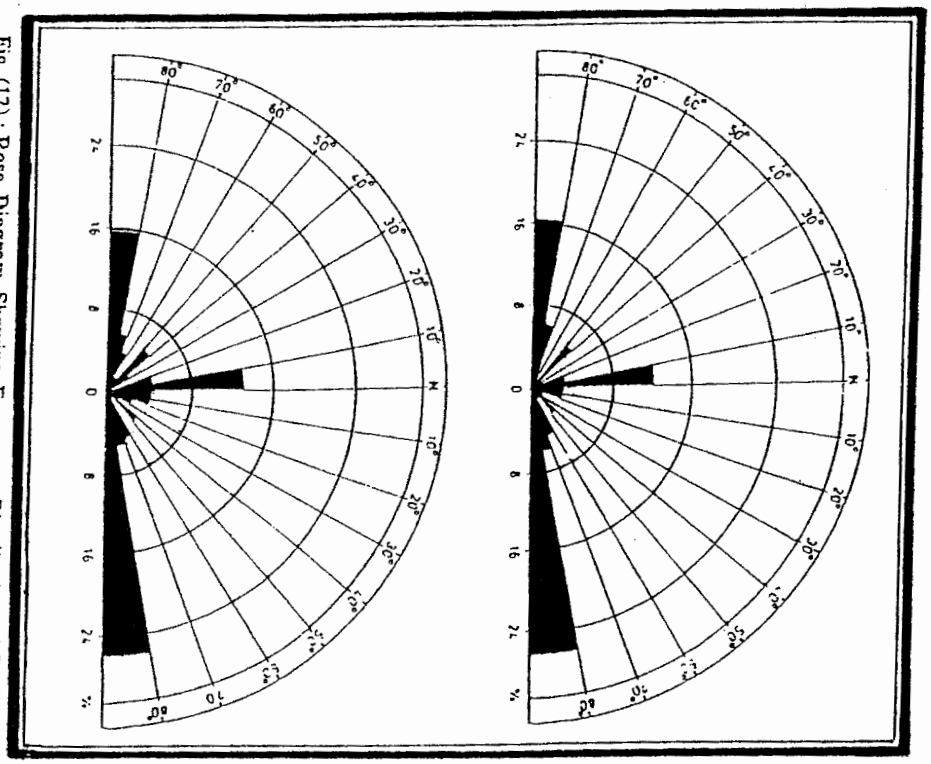

Fig. (12) : Rose Diagram Showing Frequency Distribution of Residual Magnetic Lineations in Kharga-Dakhla Oases area, Southern Western Desert, Egypt

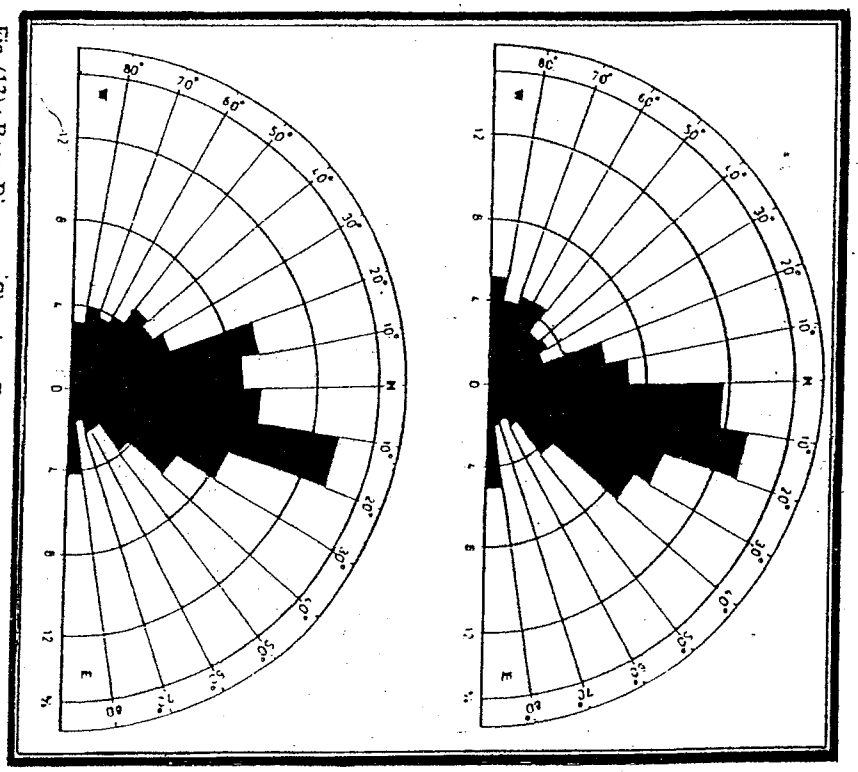

Fig. (13) : Rose Diagram Showing Frequency Distribution of Photo-Lineations in Kharga-Dakhla Oases area, Southern Western Desert, Egypt

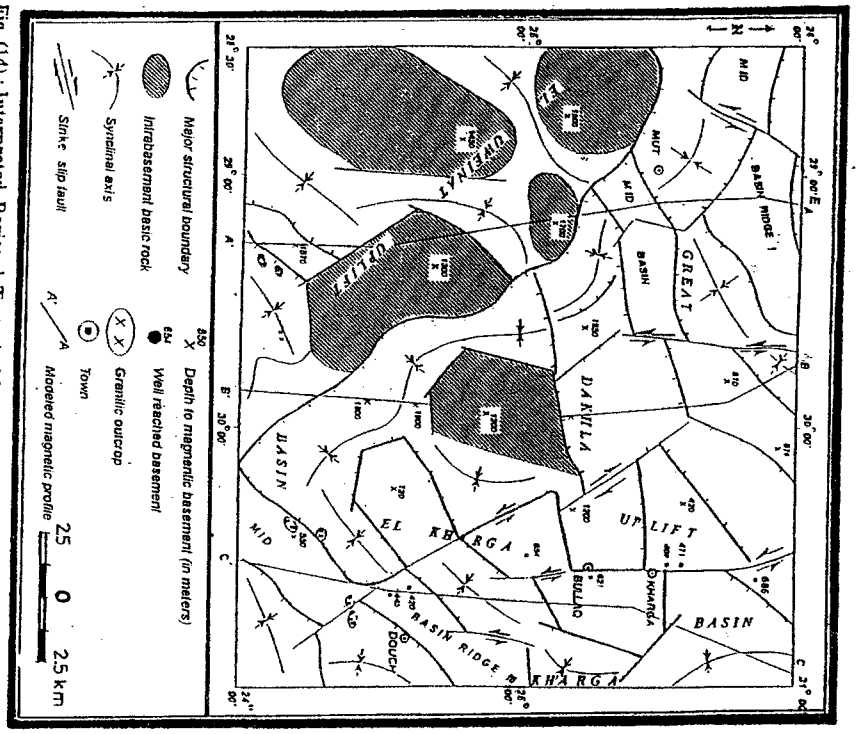

Fig. (14) : Interpreted Regional Tectonic Map of the Magnetic Basement Rocks in Kharga-Dakhla Oases area, Southern Western Desert, Egypt

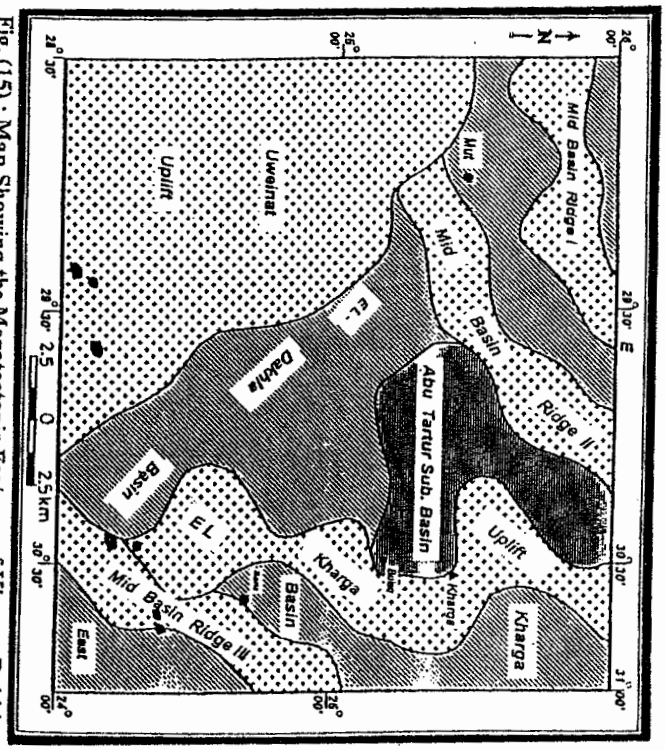

Fig. (15) : Map Showing the Megatectonic Features of Kharga-Dakhla Oases area, Southern Western Desert, Egypt

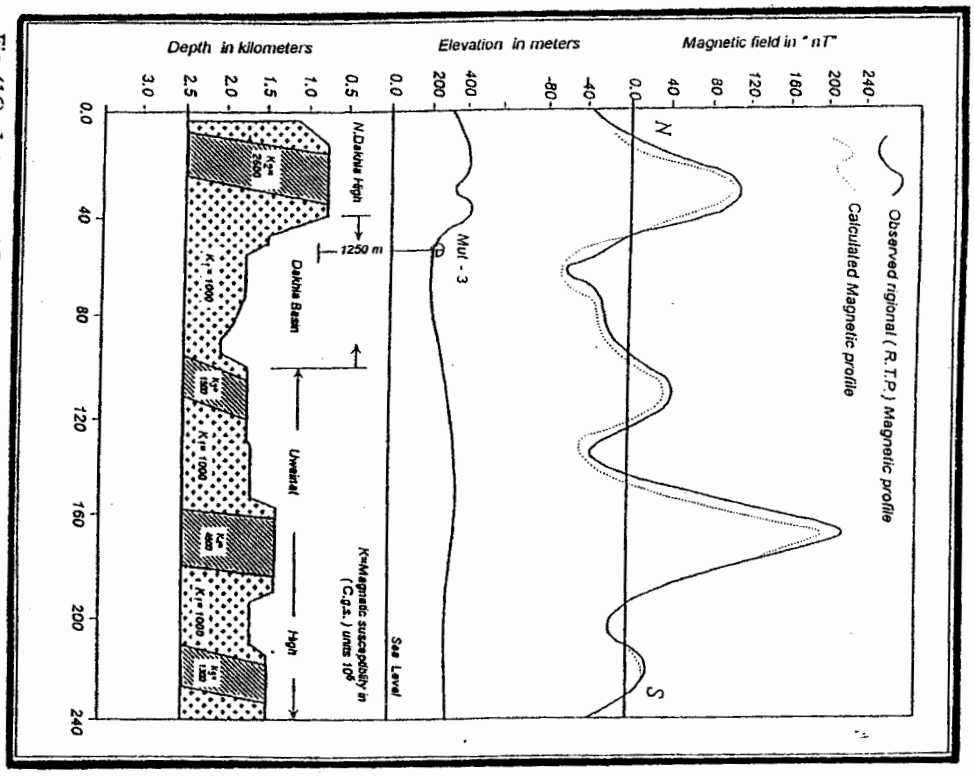

Fig. (16) : Interpreted Basement Structural Cross-Section (A-A') based on Two-Dimensional Modelling of Aeromagnetic Data in Kharga-Dakhla Oases area, Southern Western Desert, Egypt

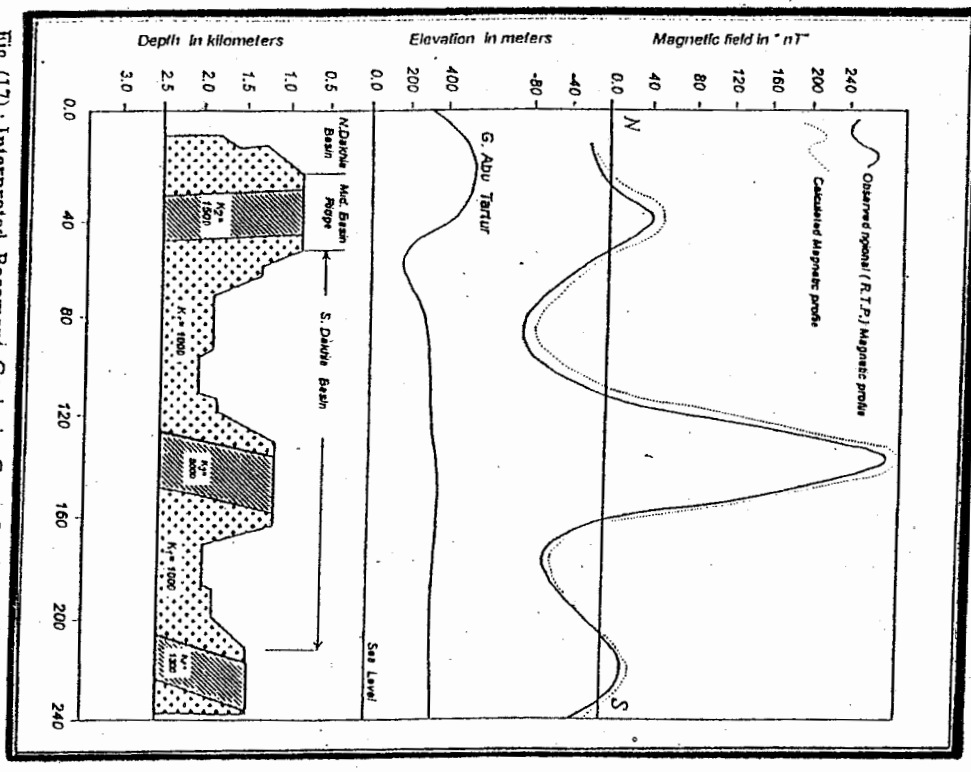

Fig. (17) : Interpreted Basement Geologic Cross-Section (B-B') based on Two-Dimensional Modelling of Aeromagnetic Data in Kharga-Dakhla Oases area, Southern Western Desert, Egypt

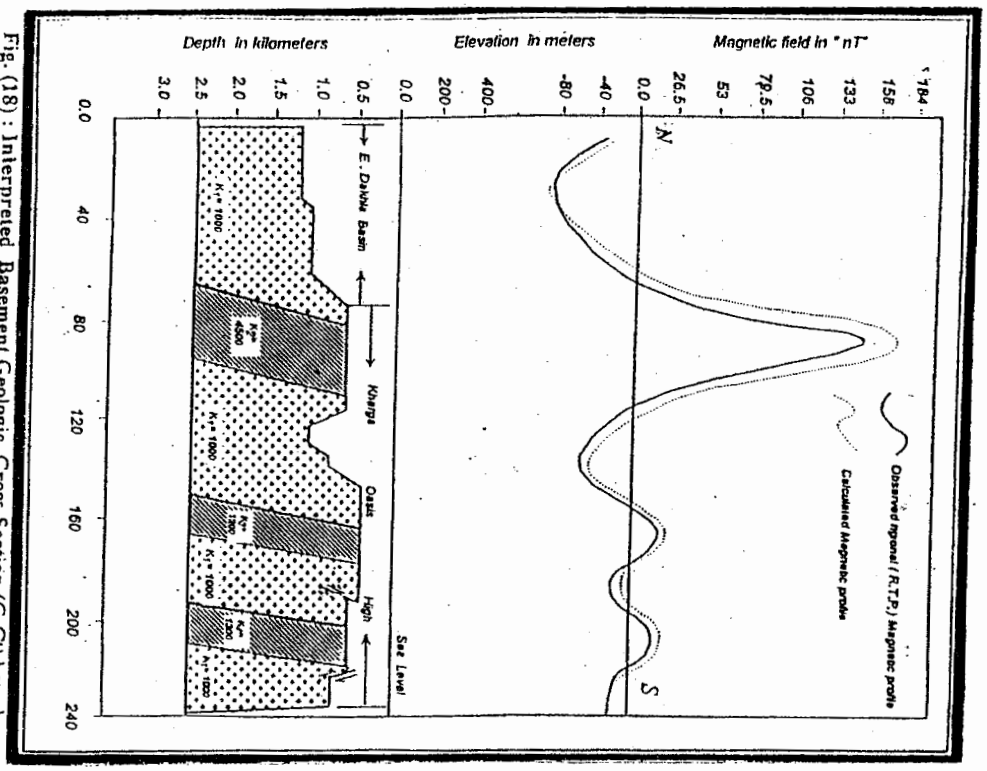

Fig. (18) : Interpreted Basement Geologic Cross-Section (C-C') based on Two-Dimensional Modelling of Aeromagnetic Data in Kharga-Dakhla Oases area, Southern Western Desert, Egypt